

# DIURNAL HEATING IN THE OKHOTSK SEA UNDER ANTICYCLONIC CONDITIONS: MULTISENSOR STUDY

Leonid Mitnik<sup>1</sup>, Anatoly Alexanin<sup>2</sup>, Maia Mitnik<sup>1</sup>, and Marina Alexanina<sup>2</sup>

<sup>1</sup> V.I. Il'ichev Pacific Oceanological Institute, FEB RAS, E-mail: mitnik@poi.dvo.ru

<sup>2</sup> Institute of Automation and Control Processes, FEB RAS, E-mail: aleks@satellite.dvo.ru

**ABSTRACT.** Development of diurnal warming in the open Okhotsk Sea during the daytime and calm conditions was studied using sea surface temperature (SST) fields retrieved from NOAA AVHRR, Terra and Aqua MODIS, Aqua AMSR-E and ADEOS-II AMSR data. Sea surface wind fields were estimated from AMSR-E/AMSR measurements as well as were obtained from QuikSCAT scatterometer. Weak winds and cloudless conditions were observed in the central area of anticyclone, which moved slowly on 28-30 June 2003 east off Sakhalin. The area where the amplitude of the diurnal SST signal  $\Delta T$  was significant also shifted slowly and had or circular or elongated shape. The  $\Delta T$  was estimated relative to the SST values in the areas surrounding the centre of anticyclone where wind speed  $W$  exceeded 5-6 m/s. The diurnal variations of SST, day-night differences were computed using NOAA-12 and NOAA-16 AVHRR-derived data. Analysis of simultaneous SST and  $W$  fields showed that the increase of  $W$  from 0 to 5-6 m/s causes the decrease of  $\Delta T$  to zero. Maximum warming exceeded 8°C and was observed in the centre of anticyclone where  $W = 0$  m/s. So strong heating was likely due to the increased chlorophyll  $a$  concentration in the area under study that follows from analysis of satellite ocean colour data.

**KEY WORDS:** Diurnal heating, SST, Wind speed, AMSR-E/AMSR, Terra/Aqua MODIS

## 1. INTRODUCTION

In calm weather conditions, the diurnal warming may significantly influence the SST. Cornillon and Stramma (1985) studied the distribution of the diurnal warming events in the Sargasso Sea using infrared measurements from NOAA satellites. In some regions, the temperature difference between the day and night measurements of SST reached 4°C. The maximum frequency of the large diurnal warming events in the Sargasso Sea was observed in June, July, and August. Even more amplitude of diurnal heating of the ocean surface exceeding 6.6°C was measured off northern California using a combination of *in situ* and NOAA-6,-7 AVHRR infrared data (Flament et al., 1994). The two warm pools were observed in a fairly clear waters corresponding Jerlov type Ia or II and was not characterized by large phytoplankton concentration. The large diurnal warming events were correlated in space with the regions of low wind speed conditions, since wind mixing of the upper ocean distributes the warming over a deeper layer and, therefore, reduce the surface temperature deviation. It was demonstrated later in a global scale by analysis of ten years of NOAA AVHRR infrared data by subtraction of nighttime SSTs from adjacent daytime SSTs (Stuart-Menteth and Robinson, 2003). TRMM-derived fields of SST and  $W$  covering four-year period allowed estimating correlation between them in the tropical areas. The amplitude of the diurnal heating  $\Delta T = T_{\text{day}} - T_{\text{night}}$  decreases exponentially with the increase of wind speed (Gentemann et al. 2003). In this study we present a detailed case study of diurnal heating event in the Okhotsk Sea. The study is based on analysis of SST and  $W$  fields retrieved from microwave and infrared measurements carried out by different sensors installed on several satellites, which sensed the

area under study several times per day when a large anticyclone was located over the Okhotsk Sea. Additional information included fields of total water vapour content of the atmosphere, cloud images, and surface analysis maps.

## 2. DATA

Diurnal warming was studied by analysis of satellite infrared and microwave measurements over the Okhotsk Sea taken under anticyclonic conditions, which were observed since 28 June till 1 July 2003. SST fields were retrieved by application of MCSST/NESDIS algorithm to infrared brightness temperatures measured by NOAA-12 and NOAA-16 AVHRR. Four or more data sets were processed every day. The sensing was carried out at about 7 and 9 UTC (local day, delay relative local time 10 hours) and at about 19 and 20 UTC (local night). The fields of SST and sea surface wind  $W$  were retrieved from the brightness temperatures measured by ADEOS-II AMSR and Aqua AMSR-E microwave radiometers by application of regression algorithms (Mitnik and Mitnik, 2003). The area under study was within a swath width of AMSR at about 1 and 12 UTC and within a swath width of Aqua at about 3 and 16 UTC. The surface wind maps were downloaded from the QuikSCAT web site. They were released two times a day: approximately at 8-9 UTC (a local evening map) and at 18-20 UTC (a local morning map), that is close to the primary synoptic dates of 06 and 18 UTC. Cloudiness was traced by the visible and infrared images received by the NOAA series AVHRR radiometer, and also by Terra and Aqua MODIS spectroradiometer. Additionally, the surface weather maps of the Japan Meteorological Agency (JMA) were used for analysis.

### 3. RESULTS

28 June – 1 July 2003 weather conditions over the Okhotsk Sea were determined by summer anticyclogenesis. Slightly-moving core of high pressure was outlined by two surface isobars. Anticyclone extended on the almost whole Okhotsk Sea. The location of its center on the surface analysis maps of the JMA was within the area 52°N-49°N, 146°E -149°E. Surface pressure in the center  $P_{max}$  varied in the limits 1010-1014 mb.

The SST field retrieved from NOAA-16 AVHRR taken on 28 June at 19:33 UTC was chosen as the references one. In the centre of anticyclone  $P_{max} = 1012$  mb, the SST values ranged from about 7°C till about 8°C and the total atmospheric water vapour content  $V = 13-16$  kg/m<sup>2</sup>. The elongated broad cloud bands were visible to the south of 51°N where  $V$  values increased to 20-23 kg/m<sup>2</sup>. Wind speed did not exceed 2-3 m/s in the large area between 52-55°N and 146-150°E as follows from QuikSCAT data and from Aqua AMSR-E measurements.

Low winds were observed on 29 June too. The absence of clouds, low winds, large duration of day (16 h 30 min) and high sun's elevation (62°) favoured intensive warming of the upper layer of the sea water. Figure 1 shows a map of diurnal warming constructed by subtraction of SST map for 28 June at 19:33 UTC (night) from SST map for 29 June at 06:56 UTC (day). Maximum warming reaches 9°C in a small circular area centred at 52.1°N, 146.8°. It is surrounded by almost concentric areas where diurnal warming decreases till insignificant level. Appearance of red bands in the bottom of the image was caused by cloud bands with temperature of their

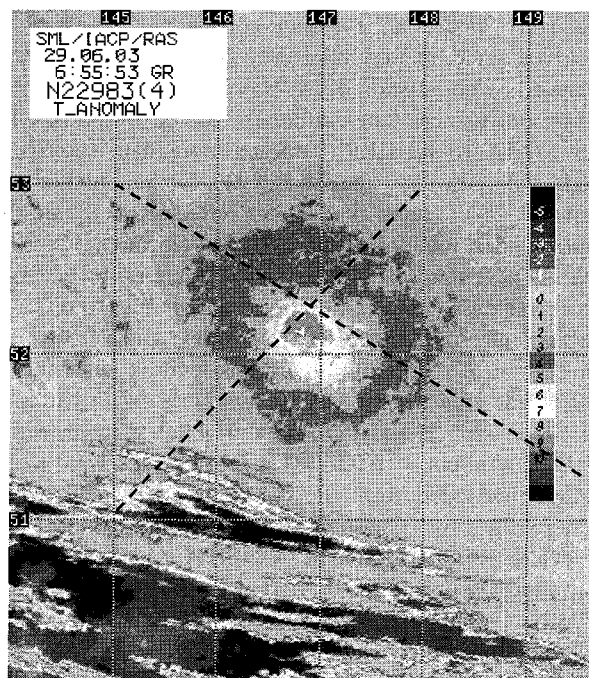


Figure 1. Diurnal warming in the Okhotsk Sea to the east of Sakhalin on 29 June 2003. Warm pool is centred near 52°N, 147°.

upper boundary about of 3-5°C that was observed in night image but was absent in day image. Variations of SST along two sections between 53°N, 148°E and 51°N, 145°E and between 53°N, 145°E and 51°N, 150°E are marked by dotted lines in Figure 1 and shown in Figure 2. Profiles of red circles cut the central area with the highest temperature measured by NOAA-12 AVHRR at 06:56 UTC (local day) on 29 June. Profiles of grey squares correspond to SST distribution along the same sections during previous local night (NOAA-12 at 19:32 UTC on 28 June). Profiles of green triangles characterize SST variations measured during next local night (NOAA-12 at 19:08 UTC on 29 June).

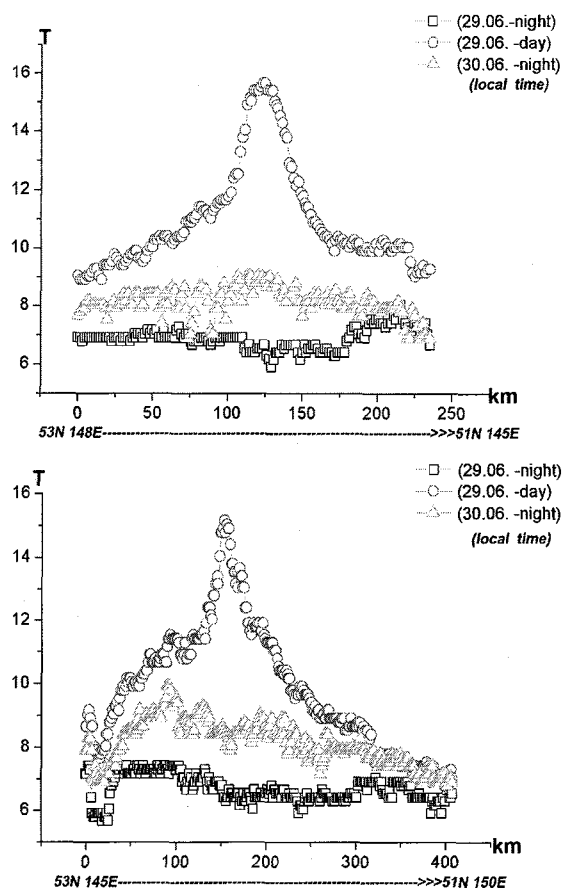


Figure 2. Temperature along the sections crossing the diurnal warming area and overlaid on Figure 1 (see text).

One of the main factors which determine amplitude of diurnal warming signal is wind speed. The areas of weak winds in the area under study were clearly distinguished on the morning and evening wind maps produced by processing of QuikSCAT scatterometer data taken on 29 June. At the same day the  $W$  and SST fields were retrieved simultaneously from AMSR-E data obtained at 03:42 UTC that was close to time of maximal diurnal heating (Figure 3). The centre location and the central symmetry of SST field in Figure 3a are the same as in Figure 1 however the presence of wind field (Figure 3b) allows to estimate relationship between SST and  $W$ .

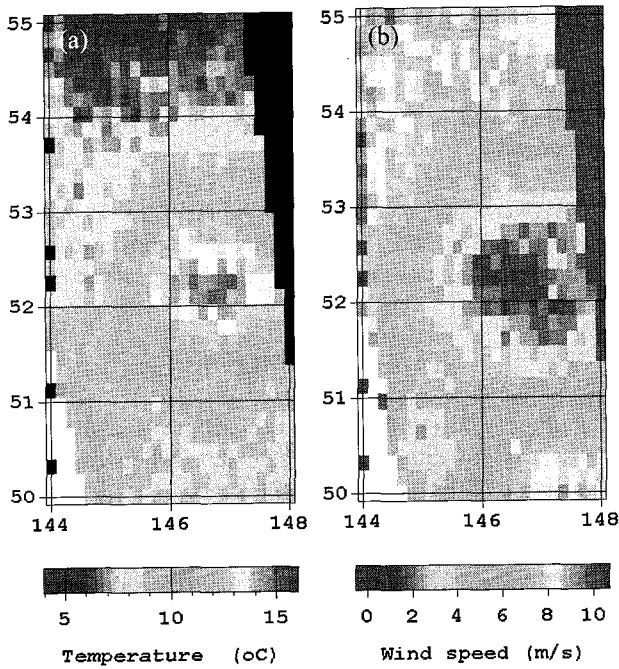


Figure 3. Maps of sea surface temperature (a) and surface wind speed (b) from Aqua AMSR-E measurements taken on 29 June at 03:42 UTC.

A scatterplot of SST versus wind speed is shown in Figure 4. SST and  $W$  pixels in the area between 50.5 and 54°N, 144.5 and 148°E for which  $W \leq 7.5$  m/s were used to generate this graphic. A red curve in Figure 4 represents an exponential approximation:  $SST = 14.3 \exp(-0.084W)$ . Under low wind speed conditions SST decreases on about 1-1.2°C with the increase of wind speed on 1 m/s.

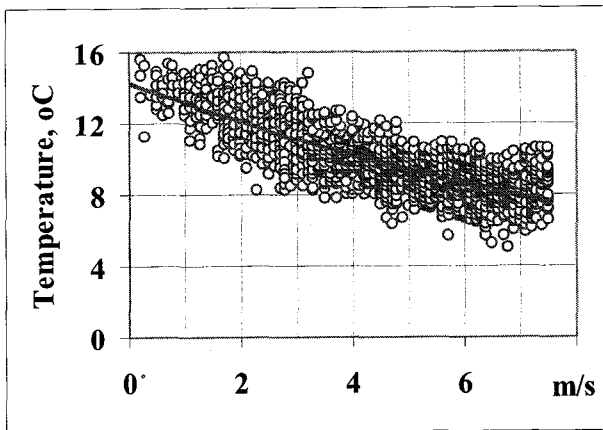


Figure 4. A scatterplot of SST versus wind speed values retrieved from Aqua AMSR-E measurements acquired on 29 June at 03:42 UTC over almost stationary anticyclone east off Sakhalin.

Concentration of chlorophyll  $a$  in the area under study was characterized by strong spatial variability (Figure 5) and varied between 0.5 and 1.0  $\text{mg}/\text{m}^3$  (as was determined from SeaWiFS data) that also could increase water temperature.



Figure 5. Aqua MODIS visible image taken on 29 June at 03:42 UTC.

A calm cloudless weather was observed next day that led to another intensive warming. Figure 6 represents a map of diurnal signal based on NOAA AVHRR data and constructed by subtraction of SST map for 29 June at 19:06 UTC (local night) from SST map for 30 June at 06:32 UTC (local day). The area of diurnal heating is elongated from the southwest to the northeast. Its width is about 250-300 km and length exceeds 600 km. The area of maximum warming where  $\Delta T \geq 7^\circ\text{C}$  also had elongated shape.

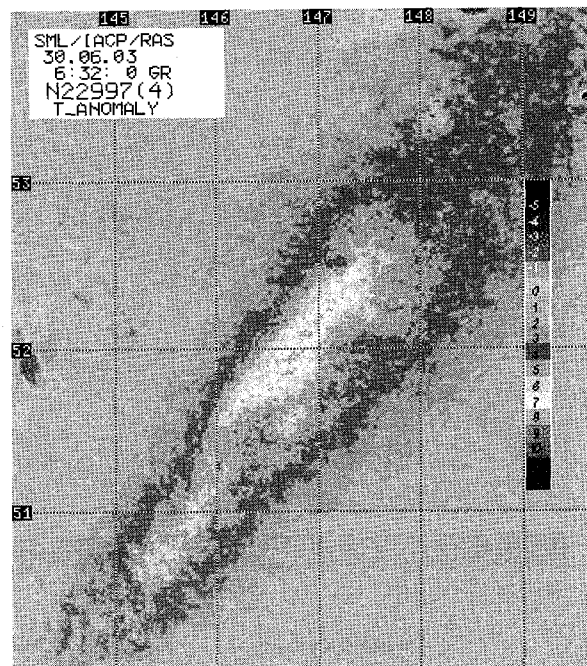


Figure 6. Diurnal warming in the Okhotsk Sea to the east of Sakhalin on 30 June 2003.

Results of AVHRR infrared data processing depicted in Figure 6 agree closely with the ADEOS-II AMSR data. Fields of SST and  $W$  retrieved from the measured brightness temperatures at frequencies 6.9 and 10.7 GHz with vertical and horizontal polarization are given in Figure 7. Diurnal warming (Figure 7a) covers a large elongated area corresponding closely to the area of low winds (Figure 7b). The considered area is characterized by the decreased values of total atmospheric water vapour content ( $14\text{-}16\text{ kg/m}^2$ ) also found from AMSR data.

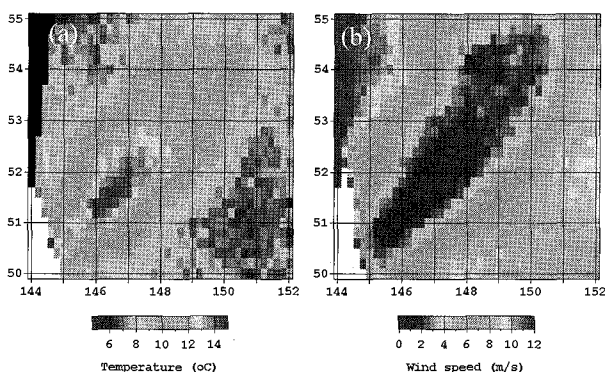


Figure 7. Maps of sea surface temperature (a) and surface wind speed (b) from ADEOS-II AMSR measurements taken on 30 June at 00:46 UTC.

The presence of large area with weak winds was confirmed by QuikSCAT scatterometer data Figure 8).

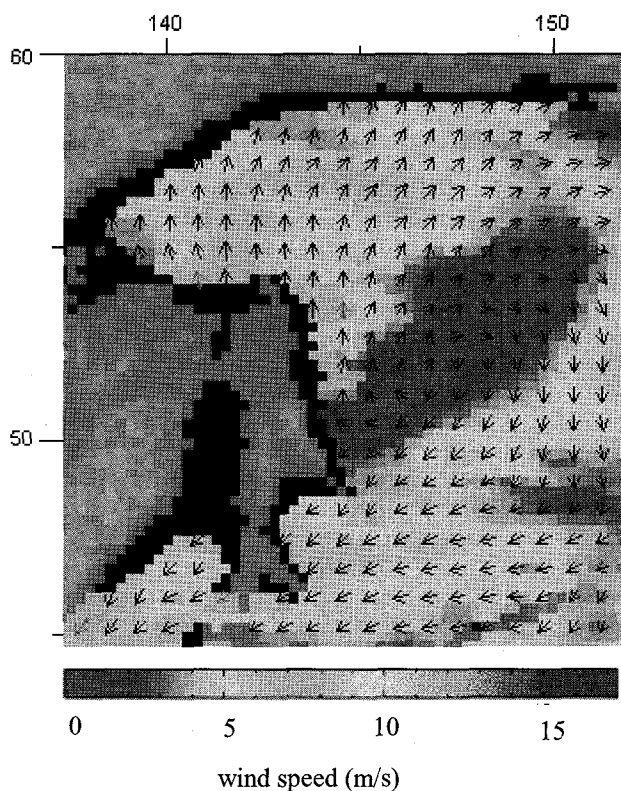


Figure 8. QuikSCAT-derived wind field over the Okhotsk Sea on 30 June 2003.

The spatial extent of low winds found on 30 June by passive (Figure 7b) and active (Figure 8) microwave instruments are practically the same. Dependence of the SST on wind speed is described by an exponential function with exponent  $\alpha = 0.069$ .

The warming patches in the Okhotsk Sea were also detected on 28 June, 1 and 2 July 2003 however their amplitudes were less than the  $\Delta T$  values measured on 29 and 30 June.

#### 4. CONCLUSIONS

Satellite multisensor data were used to document an intense case of diurnal heating in the Okhotsk Sea off Sakhalin on 28 June – 1 July 2003.

The warming area was formed in the centre of almost stationary anticyclone under exceptional combination of favourable environmental conditions: the absence of cloudiness, large duration of light day and the period of low wind speed, decreased total atmospheric water vapour content and increased plankton concentration. As a result the amplitude of the diurnal cycle of surface temperature estimated from satellite infrared and microwave measurements reached  $7\text{-}9^\circ\text{C}$  on 29-30 June. The amplitude of the diurnal warming falls off  $\exp(-\alpha W)$  where  $\alpha = 0.07\text{-}0.085$ .

#### References

- Cornillon, P., and L. Stramma, 1985. The distribution of diurnal warming events in the Western Sargasso Sea. *J. Geophys. Res.*, 90(C14), pp. 11811-11815.
- Flament, P., J. Firing, M. Sawyer, and C. Trepois, 1994. Amplitude and horizontal structure of a large diurnal sea surface warming event during the Coastal Ocean Dynamic Experiment. *J. Phys. Oceanography*, 24(1), pp. 124-139.
- Gentemann, C.L., C.J. Donlon, A. Stuart-Menteth, and F.J. Wentz, 2003. Diurnal signals in satellite sea surface temperature measurements. *Geophysical Res. Lett.*, 30(3), 1140, doi:10.1029/2002GL016291.
- Mitnik, L.M., and M.L. Mitnik, 2003. Retrieval of atmospheric and ocean surface parameters from ADEOS-II AMSR data: comparison of errors of global and regional algorithms. *Radio Sciences*, 38(4), 8065, doi: 10.1029/2002RS002659.
- Stuart-Menteth, A.C., and I.S. Robinson, 2003. A global study of diurnal warming using satellite-derived sea surface temperature. *J. Geophys. Res.*, 108(C5), 3155, doi: 10.1029/2002JC001534.

#### Acknowledgements

This study has been carried out within the cooperation between the Japan Aerospace Exploration Agency and the POI FEB RAS in the ADEOS-II Research activity (project AD2-3rdRA-ENTRY-AMSR013). This work is partially sponsored by a RFBR DVO grant 06-05-96076.